Pendellösung intensity-beat measurements with 0.0392- and 0.0265-Å γ radiation in silicon

Hans A. Graf and Jochen R. Schneider
Hahn-Meitner Institut, Glienicker Strasse 100, D-1000 Berlin 39, Federal Republic of Germany
(Received 1 May 1986)

The integrated reflecting power of the silicon (220) reflection has been measured with 316.5- and 468.06-keV γ radiation from ^{192}Ir in symmetrical Laue geometry on ⟨001⟩ floating-zone-grown single crystals of approximately 1 cm thickness and 10 cm diameter. By tilting the crystal around the scattering vector the effective sample thickness was increased in steps of about $\frac{1}{20}$ of a Pendellösung length and typically five Pendellösung oscillations were observed. After an independent determination of the sample thickness the structure factor was deduced from fitting the expression for Pendellösung intensity beats from dynamical diffraction theory to the experimental data. Using the values of the Si lattice parameter and the Debye-Waller factor from an x-ray Pendellösung study by Aldred and Hart [Proc. R. Soc. London, Ser. A **332**, 223 (1973); **332**, 239 (1973)] we obtain $F_{220}=69.16\pm0.03$ for $\lambda=0.0392$ Å and 69.21 ± 0.06 for $\lambda=0.0265$ Å, which is in excellent agreement with the x-ray value of 69.21 ± 0.06. This result justifies the use of the Thomson cross section to describe the intrinsic interaction in Bragg diffraction experiments with short-wavelength γ radiation.

I. INTRODUCTION

In the angular range where Bragg diffraction occurs, a monochromatic x-ray or neutron beam excites in a perfect crystal two interfering wave fields with different wave vectors defined by the branches of the dispersion surface. This difference is much smaller than the length of the wave vectors. In Laue (transmission) geometry it leads to a pronounced fine structure in the diffraction pattern as well as to oscillations of the intensity of the diffracted beam with sample thickness.[1] The period of these oscillations is called the Pendellösung length and is of the order of 1 mm for γ-ray diffraction in silicon. Pendellösung phenomena are of great importance for the interpretation of x-ray topographs;[2] they are not restricted to completely perfect crystals. A theory of Pendellösung fringes in distorted crystals was developed by Kato[3] and applied to Laue diffraction of x rays in homogeneously bent crystals. It was verified experimentally by Hart[4] for various degrees of sample deformation by applying a temperature gradient normal to the Bragg planes of a wedge-shaped specimen of effectively perfect silicon.

Kato and Lang[5] proposed to determine absolute structure factors from Pendellösung fringe patterns produced by wedge-shaped perfect crystals because this method is free from the ambiguity of extinction, which often limits the accuracy of structure factors measured by conventional x-ray diffraction techniques on imperfect single crystals. Because large perfect crystals are needed most Pendellösung fringe studies have been carried out on silicon samples. Aldred and Hart[6] determined a complete set of highly accurate structure factors which allowed for a detailed discussion of the electronic charge distribution in crystalline silicon. By analyzing the fine structure of Laue rocking curves Teworte and Bonse[7] determined 16 structure factors of silicon which agree well with the earlier data obtained with the Pendellösung method using wedge-shaped crystals, but probable errors were reduced to below the 0.1% level. More recently Deutsch and Hart[8] determined accurate high-order structure factors of silicon by measuring thin-crystal Laue rocking curves with a monolithic double-crystal x-ray diffractometer. Takama, Iwasaki, and Sato[9] determined structure factors from Pendellösung intensity beats measured on silicon wafers in symmetrical Laue geometry with x rays of variable wavelength from the white spectrum of an x-ray tube. The technique was applied to determine structure factors for germanium,[10] aluminum,[11] copper,[12] and zinc.[13] More recently the accuracy of the silicon (220) structure factor determined by this method was improved by analyzing Pendellösung beats at the center of the Borrmann fan on the exit surface of a silicon crystal approximately 3.4 mm thick.[14]

Pendellösung fringe studies with thermal neutrons have the advantage that absorption is very small and that the fading of the x-ray Pendellösung fringes due to the two polarization states of the electromagnetic radiation does not occur. By means of 1.18-Å neutrons Sippel, Kleinstück, and Schulze[15] measured the integrated reflecting power of the silicon (220) reflection in symmetrical Laue geometry on about 50 plane-parallel crystal plates with thicknesses varying between 6 and 204 μm. The plot of the intensities as a function of sample thickness shows the Pendellösung beats as predicted by dynamical theory for a nonabsorbing crystal. Using three silicon crystals of about 10, 6, and 3.3 mm thickness in symmetrical Laue geometry, Shull[16] measured Pendellösung beats at the center of the Borrmann fan of the (111) reflection by varying the neutron wavelength in the range between 1 and 1.2 Å in steps of approximately 0.002 Å. After application of spherical-wave theory and taking into account a uniformly curved distortion of the lattice planes in the samples the coherent nuclear scattering amplitude for silicon was determined with an accuracy of $\pm0.025\%$ from Pendellösung fringe patterns including about 20 oscillations.[17]

The problem of extinction in structure factor measurements on imperfect single crystals can be very much reduced if the diffraction experiments are performed with γ radiation from radioactive sources with wavelengths of the order of 0.03 Å.[18] In addition, absorption is as weak as in neutron diffraction, no anomalous dispersion occurs, and because of the small Bragg angles the difference in the diffraction process for the two polarization states is small and in many cases negligible. Comparison of the structure factors measured with γ radiation on simple transition metals with the results from various modern band-structure calculations reveals that the absolute scale of the experimental structure factors should be known with an accuracy of better than 0.5%.[19] This requires an experimental check of the reliability of the Thomson cross section which is used in the interpretation of the γ-ray diffraction data. The Thomson cross section is known to describe the interaction of x rays with matter perfectly well. In order to extend this statement to Bragg diffraction experiments with shorter-wavelength radiation the silicon (220) structure factor has been determined accurately from Pendellösung intensity beat measurements for 316.5- and 468.06-keV γ radiation and comparison is made with the highly accurate x-ray Pendellösung data.[6,7]

The results of dynamical diffraction theory needed to describe γ-ray Pendellösung intensity beats are summarized in Sec. II. The presentation of the experimental aspects in Sec. III includes a description of the γ-ray diffractometer used for the intensity measurements as well as a characterization of the degree of perfection of the silicon crystals. In Sec. IV the procedure to fit the experimental data to the theoretical Pendellösung intensity beats is discussed in some detail. The final results are presented in Sec. V.

II. THEORETICAL BACKGROUND

The integrated reflecting power for diffraction of x rays in transmission geometry through a plane-parallel perfect single crystal is given within dynamical diffraction theory (here we follow Ref. 20) by

$$R_{n,p}^{\mathrm{dyn}}=\frac{r_0\,|\,F_H'\,|\,e^{-W}\lambda^2 K_{n,p}}{\pi V_{\mathrm{cell}}\sqrt{|\,b\,|}\,\sin(2\theta_B)}R_{n,p}^{y}(\mathrm{Laue})\ . \tag{1}$$

n and p denote the two polarization states of the incident x-ray beam, i.e., electric field vector **E** normal or parallel to the scattering plane. r_0 is the classical electron radius. F_H' is the real part of the structure factor, e^{-W} the Debye-Waller factor, and V_{cell} the volume of the unit cell. λ represents the wavelength, $K_{n,p}$ is the polarization factor, and θ_B is the Bragg angle. b represents the ratio of the direction cosines γ_0 and γ_H and is equal to 1 for symmetric Laue geometry. $R_{n,p}^{y}(\mathrm{Laue})$ is well approximated by

$$R_{n,p}^{y}(\mathrm{Laue})\cong\frac{\pi}{2}e^{(-\mu_0 t/\gamma_0)}\left[J_0[2iA_{n,p}(k^2+g_{n,p}^2)^{1/2}]+\int_0^{2A_{n,p}}J_0(x)dx-1\right], \tag{2}$$

with

$$A_{n,p}=\frac{r_0\,|\,F_H'\,|\,e^{-W}\lambda K_{n,p}t}{V_{\mathrm{cell}}(\,|\,\gamma_0\gamma_H\,|\,)^{1/2}}\ , \tag{3}$$

$$k=\frac{F_H''}{F_H'}=\frac{\epsilon F_0''}{F_H'}\ , \tag{4}$$

$$g_{n,p}=-\frac{(1-b)\mu_0 V_{\mathrm{cell}}(1+k^2)^{1/2}}{4\sqrt{|\,b\,|}\,r_0\,|\,F_H'\,|\,e^{-W}\lambda K_{n,p}}\ , \tag{5}$$

provided $g_{n,p}\ll 1$ and $k\ll 1$. μ_0 is the linear attenuation coefficient and t represents the thickness of the crystal plate. $J_0(x)$ and $J_0(ix)$ are the zeroth order Bessel functions of the first kind for real and imaginary arguments, respectively. γ_0 and γ_H are again the direction cosines for the incident and emergent beams relative to the crystal surface. F_H'' is the imaginary part of the structure factor ($F_H=F_H'+iF_H''$), and ϵ the ratio of the imaginary part of the structure factor for a given Bragg peak relative to its value in forward direction. Equation (2) has been derived by dropping terms of the order of k^2 and g^2 compared with unity. For symmetrical transmission geometry (i.e., $b=1$ and thus $g=0$), a first-order correction to Eq. (2) results in a change of scale of $R_{n,p}^{y}$ (Laue) by a factor of $(1+7k^2/16)$. In the following it will be shown that this correction is negligible for the diffraction of 316.5- and 468.06-keV γ radiation in silicon.

F_0'' in Eq. (4) is related to μ_0 by the optical theorem

$$\mu_0=2r_0\lambda\frac{F_0''}{V_{\mathrm{cell}}}\ . \tag{6}$$

The attenuation coefficient measured in silicon with 316.5-keV (i.e., $\lambda=0.0392$ Å) γ radiation is $\mu_0=0.25$ cm^{-1} and thus several orders of magnitude smaller than the value observed in x-ray diffraction experiments. With $\mu_0=0.25$ cm^{-1}, $F_H'=69.21$ from Ref. 6, and with the usual assumption that ϵ is close to unity one calculates from Eqs. (6) and (4) $k\simeq 0.003$ and hence a correction to the scale of Eq. (2) of the order of 5×10^{-6}, which is negligible.

For an unpolarized incident beam as used in the γ-ray experiments, both polarization states are equally likely and the diffraction patterns of the two polarization states are superimposed, which leads to minima of visibility of the Pendellösung intensity beats.[21,22] These "fading regions" occur at intervals of 0.5 $(2n+1)N_{\mathrm{osc}}$ Pendellösung oscillations, where n is a positive integer or zero and

$$N_{\mathrm{osc}}=\frac{1+|\,\cos(2\theta_B)\,|}{2(1-|\,\cos(2\theta_B)\,|\,)}\ . \tag{7}$$

For diffraction of 0.0392-Å γ radiation at the (220) reflection of silicon the Bragg angle is small, $\theta_B=0.58°$, so that N_{osc} is of the order of 5000. Thus the first minimum of visibility of the Pendellösung intensity beats (i.e., $n=0$) is expected at values of A of the order of 7500. (Oscillations of higher order than the first few have a periodicity of π on the A scale.) In Pendellösung intensity beat studies with γ radiation the maximum A value is of the order of 200 and therefore the fading of the fringe pattern due to the two polarization states can hardly be seen. The integrated reflecting power for an unpolarized beam is given

by

$$R^{\mathrm{dyn}}=\tfrac{1}{2}(R_n^{\mathrm{dyn}}+R_p^{\mathrm{dyn}}) , \tag{8}$$

where R_n^{dyn} and R_p^{dyn} are calculated separately from Eq. (1) using $K_n=1$ and $K_p=|\cos(2\theta_B)|$, respectively. In Fig. 1 R^{dyn} is plotted as a function of

$$A=\tfrac{1}{2}(A_n+A_p) \tag{9}$$

up to values of $A=120$. The difference between A and A_n, A_p is only of the order of 10^{-4}.

In order to observe such Pendellösung intensity beats experimentally, one can measure the integrated reflecting power as a function of A. For a given Bragg reflection this has been done either by varying the wavelength of the incident beam, or by varying the thickness of the sample.[23,24] The calculations shown in Fig. 1 are made for the Si (220) reflection and γ radiation of fixed wavelength $\lambda=0.0392$ Å. The variation of A from 0 to 120 corresponds to a variation of the crystal thickness from 0 to about 20 mm. If one is not especially interested in Pendellösung oscillations for values of A smaller than about 20, the variation of sample thickness can be realized simply by tilting a plate-shaped crystal of thickness of a couple of mm around the scattering vector.

III. EXPERIMENTAL

A. γ-ray diffractometer

Pendellösung intensity beats were measured on silicon single crystals by the γ-ray diffractometer installed at the Hahn-Meitner-Institut. This diffractometer works with a commercially available ^{192}Ir γ-ray source of 200 Ci activity and a half-life of 74.2 days. The energy width of the γ-ray lines is only $\Delta E/E\cong 10^{-6}$ and, thus, the resolution of the instrument is solely determined by the angular divergence of the incident beam, which is controlled by two lead collimators. In the present experiments, two γ lines of $E=316.5$ and $E=468.06$ keV, corresponding to wavelengths of 0.0392 and 0.0265 Å, respectively, were used and the horizontal divergence was chosen to be 3.4 min of arc, selecting a collimator of 2×4 mm^2 rectangular cross section for defining the beam in front of the sample. The sample is mounted in a large Huber χ-ϕ circle which is attached to a turntable allowing ω scans in steps of $\frac{1}{4000}$ of a degree. In addition, the whole sample goniometer can precisely be translated in horizontal and vertical directions with respect to the incident beam. The adjustment of the sample is checked by a laser, which is set up opposite to the source, several meters away from the sample, with its beam in line with the γ-ray beam. An intrinsic Ge solid-state detector serves to measure the diffracted and the transmitted beam. The various γ lines are discriminated electronically. A detailed description of the diffractometer is given in Ref. 25.

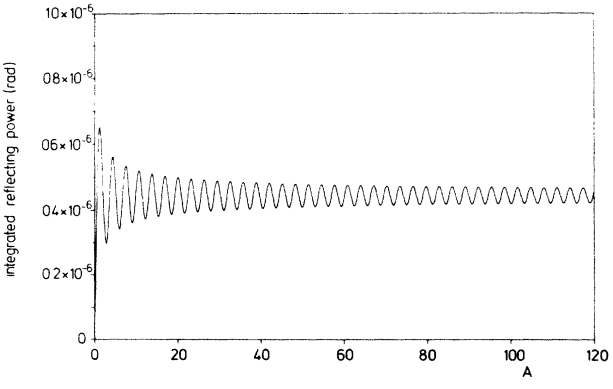

FIG. 1. Integrated reflecting power for diffraction of 0.0392-Å γ radiation at silicon (220) calculated from dynamical theory [Eq. (1)] as a function of the parameter A defined in Eq. (3).

B. Samples and the sample mounting

Two floating-zone-grown silicon single crystals, in the following referred to as crystal I and II, were kindly provided by Wacker-Chemitronic, Burghausen, Federal Republic of Germany. Both crystals had the shape of a disk approximately 100 mm in diameter and 10 mm in thickness. They were cut with their surfaces parallel to the (001) plane from cylinders grown in the ⟨001⟩ direction. The surfaces were chemically polished. Crystal I had been produced by an improved growth technique, where the parameters affecting the convection in the melt had been changed compared with the standard Wacker floating-zone technique, for which crystal II is an example. The residual resistivity was 20.8 Ω cm for sample I and 8.2 Ω cm for sample II. The thickness of sample I was measured at the Bundesanstalt für Materialprüfung in Berlin to $T_0=9.4871\pm 0.0006$ mm using the digital, optoelectronic calliper MT30 of the company Heidenhain. In the area of interest the crystal surfaces showed a ripple of ± 1 μm.

The samples were mounted on a goniometer head using specially shaped aluminum rings, the inner surfaces of which were coated with wax. The crystals were put into these rings without applying pressure and were fixed there by slightly warming up the whole ensemble with hot air, and subsequently cooling it down. By this technique it was ensured that elastic strains, introduced by the mounting of the crystals, were minimized. The ϕ shaft of the χ-ϕ circle, to which the goniometer head was attached, was positioned at $\chi=90°$ and the scattering vector of the Bragg reflection to be measured was oriented collinear to the ϕ axis in the usual way, using the two arcs of the goniometer head. By ϕ and ω movements of the diffractometer, the crystal disk was then put perpendicular to the laser beam and, thus, perpendicular to the γ-ray beam, with an accuracy better than 0.02°. This position defined the zero point $\Psi=0°$ for the rotation around the scattering vector, which was performed by the ϕ movement in the χ-ϕ circle. From the ω movement necessary to bring the crystal from the perpendicular position back to the Bragg position for the three different reflections measured, (400), $(2\bar{2}0)$, and (220), it could be estimated that crystals I and II were both cut perpendicular to ⟨001⟩ within 0.5°.

C. Integrated reflecting power

The basic quantity measured in the present experiments is the integrated reflecting power of a Bragg reflection in Laue geometry. This quantity was determined from ω-step scans, where the reciprocal lattice vector corresponding to a specific reflection was rotated through the Bragg condition with a step width $\Delta\omega$ of typically 0.005°. Figure 2 shows such a rocking curve from the $(2\bar{2}0)$ reflection of the crystal I at zero tilt angle ($\Psi=0°$). By tilting the crystal around the scattering vector, the effective thickness of the crystal disk is changed. Repeating the ω-step scans at various tilt angles Ψ, thus allows one to sample the integrated reflecting power as a function of the effective crystal thickness.

In order to put the measured integrated reflecting power on an absolute scale, it is necessary to determine the incident beam intensity. On the γ-ray diffractometer this is usually done by measuring the intensity of the transmitted beam, with the sample oriented just off the Bragg reflecting condition. The experimentally observed integrated reflecting power $R_H^{\rm obs}$ is then defined as the integral over the reflection curve

$$R_H^{\rm obs}=\int r_H(\omega)d\omega \ , \tag{10}$$

where $r_H(\omega)$ is the reflectivity at a particular ω position,

$$r_H(\omega)=\frac{P_H(\omega)-P_B}{P_T^*} \ , \tag{11}$$

with $P_H(\omega)$ being the diffracted intensity. As suggested by the profile shown in Fig. 2, the background intensity P_B is considered to be linear over the whole scan range. If P_0 represents the intensity of the primary beam, the transmitted intensity P_T^* is given by

$$P_T^*=P_0\exp(-\mu_0 T_0/\cos\theta_B) \ . \tag{12}$$

T_0 is the thickness of the crystal disk and μ_0 the linear attenuation coefficient. All measured intensities are corrected for the time decay of the γ-ray source, which for ^{192}Ir amounts to approximately 1% per 24 h. By normalizing the observed intensities with P_T^* rather than P_0, the $R_H^{\rm obs}$ values are experimentally corrected for absorption and have to be compared with theoretical values calculated for zero absorption.

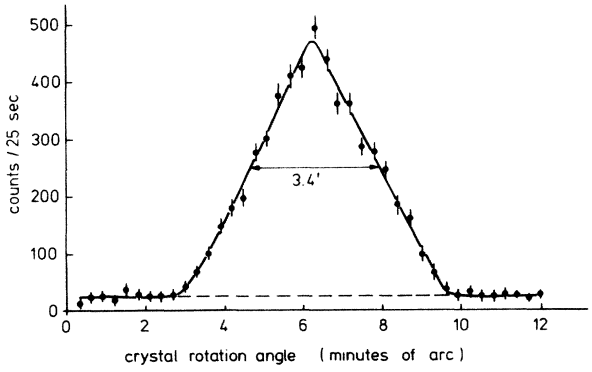

FIG. 2. Rocking curve measured with 0.0392-Å γ radiation from a 175 Ci ^{192}Ir source at silicon $(2\bar{2}0)$. The triangular shape of the pattern reflects the resolution function for the slit geometry employed on the γ-ray diffractometer.

In case of the ^{192}Ir γ-ray source, which emits several strong γ lines in the energy range between 300 and 600 keV, a careful energy analysis must be performed when determining the transmitted intensity for the 316.5- and 468.06-keV lines. Here problems especially arise from the Compton part of the pulse-height spectrum, produced in the solid-state detector by the higher energy lines, which can overlap with the energy window set to separate a given line from the others. Rather long measuring times are necessary to get high accuracy in P_T^*. In order to economize the measuring time, P_T^* was determined only once at the tilt angle $\Psi=0°$ with an accuracy of 2%, for each of the two wavelengths used in the experiments, while the error in the individual integrated reflectivity measurements was approximately 1%. The linear attenuation coefficient was determined to $\mu_0=0.25(2)$ cm^{-1} for $\lambda=0.0392$ Å and $\mu_0=0.23(2)$ cm^{-1} for $\lambda=0.0265$ Å, where the uncertainty of about 9% reflects the error of 2% in the absolute scale caused by the limited accuracy of the P_T^* value for $\psi=0°$. Using these attenuation coefficients, the P_T^* values for the other tilt angles ψ were calculated.

D. Overall characterization of the perfection of the samples

The overall perfection of both crystals was investigated by measuring the integrated reflecting power of the Bragg reflections (400), (220), and $(2\bar{2}0)$ in different sections of the two crystals and for a series of different tilt angles Ψ. The measurements were performed with 0.0392-Å radiation at nine volume elements, each separated from the other by a horizontal translation of $\Delta x=10$ mm. Starting from the perpendicular orientation with $\Psi=0°$, the crystal was rotated around the scattering vector, clockwise as well as counterclockwise, in steps of $\Delta\Psi=15°$ up to maximum tilt angles of $\Psi=+75°$ and $-75°$, respectively. The shape of the irradiated crystal sections differs from one tilt angle to another and the effective thickness increases proportional to $1/\cos\Psi$ up to about 4 times the thickness T_0 of the disk. The integrated reflecting power of perfect crystals, however, is essentially independent of the crystal thickness. According to Fig. 1, for the conditions of the present experiments one should only expect intensity oscillations around a mean value with amplitudes of the order of 10%.

The results of these measurements are shown in Fig. 3 for sample I and in Fig. 4 for sample II. Each experimental point, depicted as solid circles corresponds to the integrated reflecting power for a specific crystal volume element and a specific tilt angle Ψ. Following dynamical diffraction theory, in the scale of Figs. 3 and 4, the distribution of the experimental points should be flat. In the case of sample I this is indeed found for reflection (400) and with some minor deviations also for reflection $(2\bar{2}0)$. However, an increase of the integrated reflecting power with increasing positive as well as negative tilt angle Ψ is

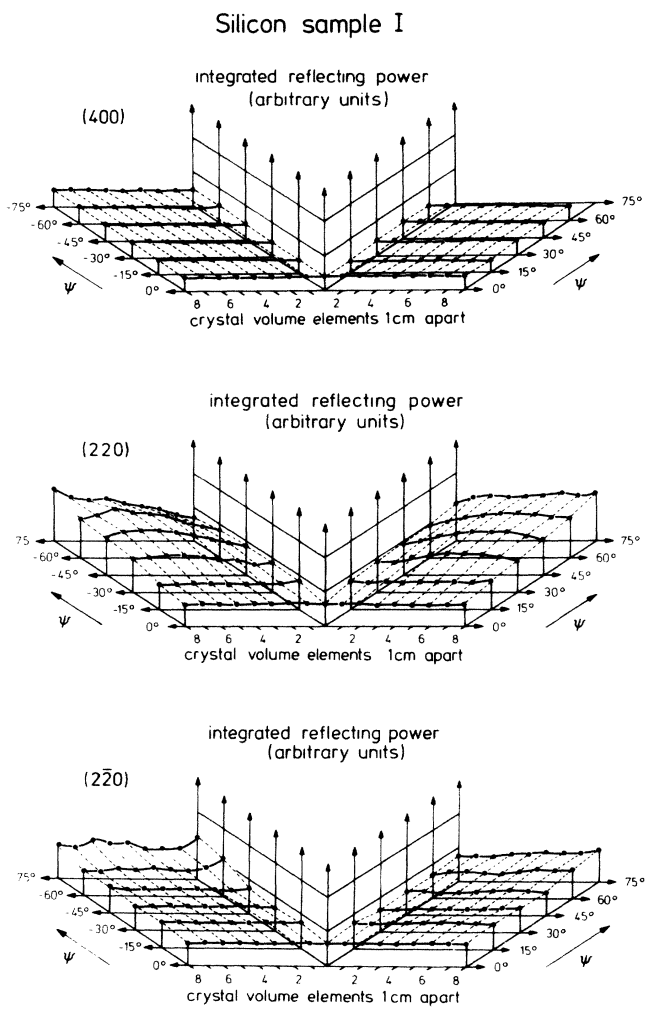

FIG. 3. Integrated reflecting power measured with 0.0392-Å radiation at reflections (400), (220), and (2$\bar{2}$0) on sample I (⟨001⟩ floating-zone-grown silicon crystal, 100 mm in diameter and approximately 10 mm thick). Nine volume elements on a line across the crystal center and separated by a horizontal translation of $\Delta x = 10$ mm have been studied. The sample was tilted around the scattering vector in steps $\Delta\Psi = 15°$ from $\Psi = 0$, where the normal of the crystal disk lies in the scattering plane, clockwise up to $\Psi = 75°$ and counterclockwise up to $\Psi = -75°$. The experimental data were corrected for absorption and time decay of the ^{192}Ir γ-ray source.

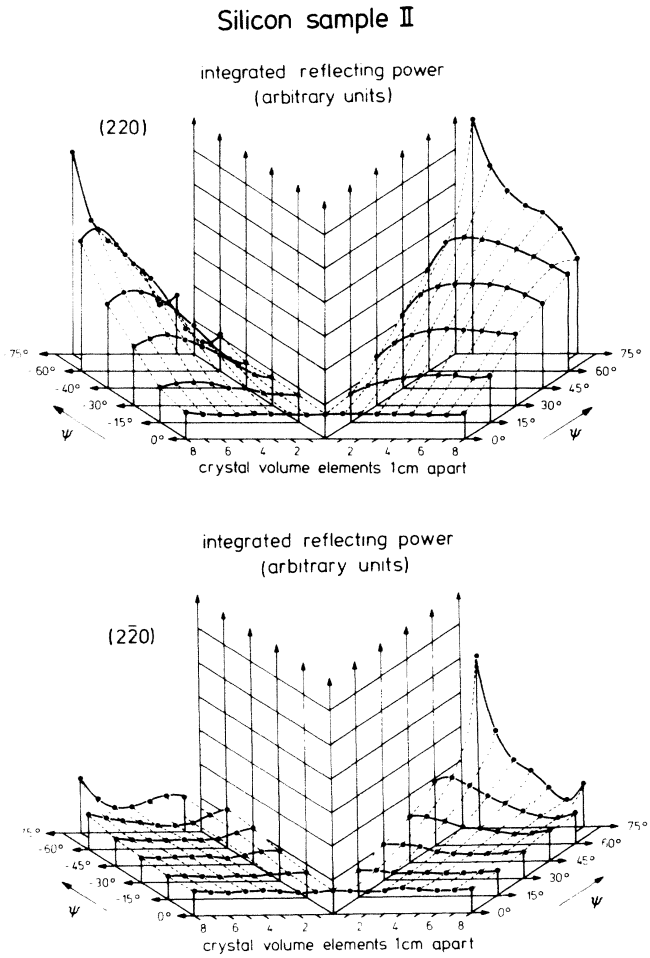

FIG. 4. Integrated reflecting power measured with 0.0392-Å radiation at reflections (220) and (2$\bar{2}$0) on sample II (see caption of Fig. 3).

observed for reflection (220), which may be due to a slight curvature of the (220) lattice planes.[26] Figure 4 demonstrates that this behavior is much more pronounced in crystal II, where especially the {220} reflections exhibit drastic changes up to a factor of 10 in the integrated reflecting power. A more detailed discussion of these features, including measurements on silicon crystals grown by the Czochralski technique with and without application of an axial magnetic field to inhibit fluid flow instabilities, will be presented elsewhere.[27] However, one aspect should be stressed here. For all three reflections and all crystals investigated the measured integrated reflecting power agreed well with the value from dynamical diffraction theory for a perfect crystal whenever the sample was oriented such that the growth direction, i.e., the normal of the crystal disk, lies in the scattering plane. This result suggests that the observed gross deviation from dynamical theory cannot be caused by surface damage. In conclusion, crystal I, which was produced by the improved floating-zone-growth technique, as a whole, behaves much more perfectly than crystal II and therefore was selected for making the detailed measurements of the Pendellösung intensity beats with γ radiation.

E. Measurement of Pendellösung intensity beats

The Pendellösung intensity beats were measured at the center of crystal I (position 4 in Fig. 3) for two wavelengths and the Bragg reflections (220) and (2$\bar{2}$0). The {220} reflections were investigated, rather than reflection (400), in order to obtain higher counting rates due to the larger structure factor. Figure 5 shows the results of the measurements performed with 0.0392- and 0.0265-Å γ radiation, respectively. Each experimental point in these figures corresponds to the integrated reflecting power R_H^{obs}, measured for a specific tilt angle Ψ and, thus, for a specific effective sample thickness t_{eff}. Starting at $\Psi = 0°$ only positive tilt angles were used. The step width in Ψ

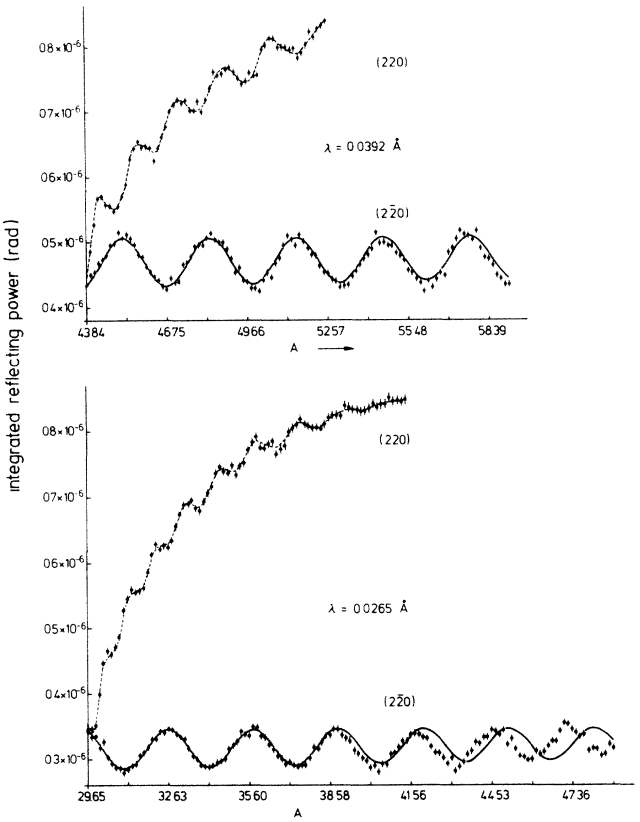

FIG. 5. Pendellösung intensity beats measured with 0.0392- and 0.0265-Å γ-radiation at reflections (220) and (2$\bar{2}$0) on sample I.

was not constant, but adjusted in such a way that the function $1/\cos\Psi$ increased with a constant step width, in order to have the experimental points equally distributed over the Pendellösung oscillations as a function of the parameter A defined in Eq. (3).

As demonstrated in Fig. 5 the integrated reflecting power from the (220) reflection increases strongly with increasing tilt angle and is modulated by oscillations of an amplitude and period much smaller than that calculated for an undistorted crystal, whereas the reflectivities measured on the (2$\bar{2}$0) reflection, i.e., after rotating the crystal around ⟨001⟩ by 90°, deviates from a curve calculated for a perfect crystal only for high tilt angles. The deviations from dynamical theory observed at (220) are more pronounced for the shorter wavelength. A shortening of the observed Pendellösung period, compared to calculations for a perfect crystal, has already been observed with x-rays and was attributed to elastic strain.[3,4] We conjecture that the samples investigated in the present γ-ray study also suffer from internal strain. The effects of the strain fields may be visualized as producing a curvature on the reflecting lattice planes, concentric to the growth direction ⟨001⟩, which affects the scattering properties the more, the larger the angle Ψ by which the growth direction is tilted out of the scattering plane. This strain field must be very anisotropic with respect to the growth direction, as can be seen from a comparison of the data measured at (2$\bar{2}$0) and (220).

IV. MODEL FITTING

The integrated reflecting powers measured at the (2$\bar{2}$0) reflection of silicon sample I, which are presented in Fig. 5, show the typical oscillations around a mean value predicted by dynamical theory. The basic parameter in this theory, A, was defined in Eq. (3). It is essentially the product of the wavelength, the crystal thickness, and the structure factor, including the Debye-Waller factor. The wavelengths of the γ radiation emitted from ^{192}Ir are known with an accuracy of the order of $\pm 2\times 10^{-5}$.[28] Thicknesses of typically 1 cm can be measured precisely and therefore it should be possible to determine the structure factor by fitting the theoretical expression given in Eq. (1) to the observed reflectivities, with $F'_H e^{-W}$ as the only variable parameter.

A. Modification due to surface damage

The calculations with Eq. (8) using the generally accepted value $F'_{220}e^{-W}=67.08$ (Ref. 6) reveal that the measured integrated reflecting powers oscillate around a mean value, which is 5% higher than the calculated one, while the amplitude of the observed and the calculated oscillations agree within statistical accuracy. This "base line shift" is too large to be explained by the uncertainties in the procedure adopted to put the measured intensities on an absolute scale. Instead, it may simply be due to surface damage. To first approximation one can assume that a thin imperfect surface layer scatters the incident radiation according to the kinematical diffraction theory, while the perfect bulk of the sample obeys dynamical theory. In order to check the validity of this assumption, calculations were performed using the following expression for the integrated reflecting power:

$$R_i^{\rm calc}=Q\frac{T_0^{\rm kin}}{\cos\theta_B\cos\Psi_i}+R_i^{\rm dyn}\ . \tag{13}$$

Here the index i denotes a calculation for a specific tilt angle Ψ_i. Equation (13) combines the dynamical scattering from Eq. (8), using $t=T_0^{\rm dyn}/\cos\Psi_i$ in Eqs. (2) and (3), with a kinematical scattering term, where Q is given by

$$Q=\frac{r_0^2\,|F'_H|^2 e^{-2W}\lambda^3}{V_{\rm cell}^2\sin(2\theta_B)}\,\frac{1+\cos^2(2\theta_B)}{2}\ . \tag{14}$$

The calculations led to a satisfactory result. In the simple model, described by Eq. (13), the total thickness T_0 of the crystal disk, measured normal to its surface, is the sum of the thicknesses of the two damaged surface layers, $T_0^{\rm kin}$, and the thickness of the perfect bulk $T_0^{\rm dyn}$,

$$T_0=T_0^{\rm kin}+T_0^{\rm dyn}\ . \tag{15}$$

By tilting the sample around the scattering vector, both the kinematical and the dynamical thickness are varied by a factor of $1/\cos\Psi_i$. It usually will not be possible to measure $T_0^{\rm kin}$ or $T_0^{\rm dyn}$ separately. These quantities are thus only accessible by a fitting procedure.

B. Fitting procedure

For computing integrated reflecting powers $R_i^{\rm calc}$, and fitting them to the corresponding reflectivities $R_i^{\rm obs}$, Eq.

(13) was implemented as a subroutine in the standard fit program MINUIT.[29] The function minimized by this program is

$$\chi^2=\sum_{i=1}^{N}\left[\frac{R_i^{\text{obs}}-R_i^{\text{calc}}}{\sigma_i^{\text{obs}}}\right]^2. \quad (16)$$

Here N is the number of observations, i.e., the number of different tilt angles Ψ_i, at which the reflectivities R_i^{obs} were measured, and σ_i^{obs} is the standard deviation of R_i^{obs}, essentially derived from counting statistics. The following quantities in Eq. (13) were defined as variables and could, in principle, be refined: F'_He^{-W}, T_0^{dyn}, T_0^{kin}, μ_0, k (anomalous dispersion), b (asymmetrical crystal cut parameter), and the product $T_0^{\text{dyn}}(F'_He^{-W})$ in the parameter A. In addition, S, a scale factor for the R_i^{obs} values, and Ψ_0, a zero-point offset applying to the tilt angles Ψ_i, were introduced as variable parameters.

In trial fits all these quantities were varied. It turned out that those parameters which essentially act as a scale factor to the experimental data, like S and μ_0, or which shift the base line of the calculated integrated reflecting power, like T_0^{kin}, k and b are highly correlated. The fitting procedure is not sensitive to these parameters. It is, however, extremely sensitive to variations of the parameter A: Adjusting the flanks of the calculated oscillation pattern to the flanks of the observed Pendellösung intensity beats is the important step in fitting the model and it proved that this can only be achieved for a sharply defined set of A values. Therefore, in the final fits with the results presented in Table I only two parameters were refined: T_0^{kin}, which mainly shifts the base line of the calculated integrated reflecting power, and the product $T_0^{\text{dyn}}(F'_He^{-W})$ in the parameter A. The other parameters were fixed at the following values: F'_He^{-W}, when occurring in the kinematical scattering term in Eq. (13) and in the prefactor in front of the oscillating function $R_{n,p}^{\nu}$(Laue) in Eq. (1) had the value 67.08.[6] At these positions, the structure factor is highly correlated with a scale factor. μ_0 was set to zero, because the R_i^{obs} values were normalized by P_T^* [Eq. (12)] and therefore have to be compared with theoretical values calculated for zero absorption. The anomalous dispersion parameter k was fixed at zero. It was discussed in Sec. II that this parameter is so small in γ-ray diffractometry, that the resulting correction term is negligible. The asymmetry parameter b was chosen to be 1. The angle of miscut was measured to be smaller than 0.5° and such minor deviations from the symmetrical Laue geometry do not affect the calculated integrated reflecting power significantly. S, the scale factor for the measured integrated reflecting powers, and Ψ_0, the zero-point offset for the tilt angle Ψ, were kept at values 1 and 0, respectively. Trial fits, where these parameters were free, did not improve the goodness of fit.

V. RESULTS AND DISCUSSION

The results of the fitting procedure are shown in Figs. 6 and 7. The solid line in Fig. 6 represents the theoretical curve obtained from a fit to the first 64 data points measured with 0.0392-Å radiation up to a tilt angle of

TABLE I. Results obtained by fitting Eq. (13) to the integrated reflecting power measured with 0.0392- and 0.0265-Å γ radiation as a function of crystal tilt angle Ψ at the $(2\bar{2}0)$ reflection of sample I. The various ranges of the tilt angle Ψ considered in the partial fits correspond to the regions A1 to A5 and B1 to B6 in Figs. 6 and 7, respectively. N is the number of data included in the partial fits and $(F'_He^{-W})T_0^{\text{dyn}}$ is the product of structure factor, Debye-Waller factor, and thickness of the perfect part of the crystal, while T_0^{kin} represents the thickness of the two damaged surface layers. The goodness of fit, GOF, is $\chi^2/(N-p)$, with p the number of parameters, and R is $100[\chi^2/\sum_{i=1}^{N}(R_i^{\text{obs}}/\sigma_i^{\text{obs}})^2]^{1/2}$. These are the usual quantities to describe the quality of a fit.

Tilt range	N	$(F'_He^{-W})T_0^{\text{dyn}}$	T_0^{kin} (μm)	GOF	R (%)
Diffraction of 0.0392-Å γ radiation at Si $(2\bar{2}0)$					
$0\le\Psi\le20.32$	21	635.75±0.23	6.42±0.22	1.01	0.85
$20.80\le\Psi\le28.33$	21	635.51±0.23	6.11±0.20	2.08	1.23
$28.64\le\Psi\le34.21$	22	635.51±0.22	4.90±0.19	2.45	1.35
$34.44\le\Psi\le38.37$	20	636.03±0.22	4.51±0.19	1.17	0.92
$38.56\le\Psi\le42.14$	22	636.74±0.19	4.84±0.17	5.33	1.98
$0\le\Psi\le34.21$	64	635.58±0.13	5.73±0.12	2.29	1.34
Diffraction of 0.0265-Å γ radiation at Si $(2\bar{2}0)$					
Tilt range	N	$(F'_He^{-W})T_0^{\text{dyn}}$	T_0^{kin} (μm)	GOF	R (%)
$0\le\Psi\le29.64$	31	635.74±0.34	7.50±0.37	1.12	1.30
$30.07\le\Psi\le37.53$	22	636.73±0.39	7.34±0.38	0.87	1.12
$37.82\le\Psi\le42.50$	18	637.52±0.37	5.29±0.38	0.86	1.10
$42.73\le\Psi\le46.65$	20	640.06±0.36	4.47±0.34	1.23	1.34
$46.83\le\Psi\le49.73$	18	643.42±0.34	5.92±0.33	1.43	1.40
$49.89\le\Psi\le52.76$	21	648.44±0.38	8.35±0.29	4.50	2.48
$0\le\Psi\le34.32$	43	635.90±0.28	7.75±0.29	1.11	1.30

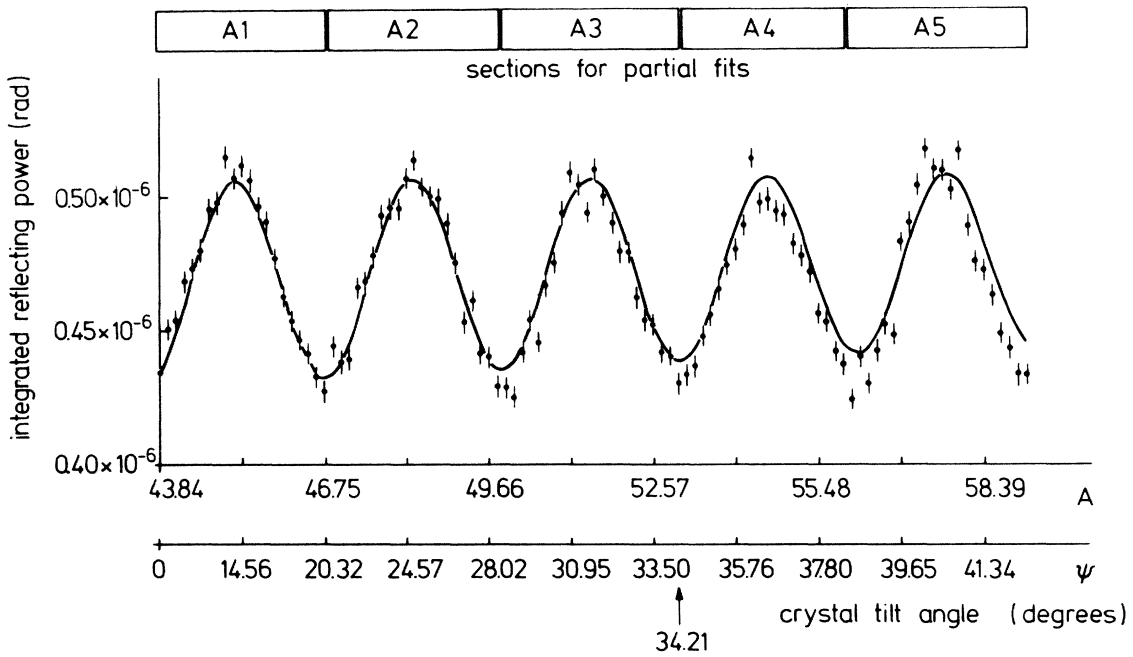

FIG. 6. Integrated reflecting power measured with 0.0392-Å γ radiation at the $(2\bar{2}0)$ reflection of sample I. The experimental data are corrected for absorption and time decay of the γ-ray source. They are plotted as a function of the parameter A, as well as the tilt angle Ψ. The solid line represents the final result from the fit of Eq. (13) to 64 data points up to $\Psi=34.21°$.

$\Psi=34.21°$. The data measured at higher tilt angles are shifted towards smaller A values, i.e., the experimental Pendellösung period gets shorter with increasing Ψ, which indicates an increasing internal strain. The same behavior was observed for the measurements with $\lambda=0.0265$ Å shown in Fig. 7. Here the solid line represents the theoretical curve fitted to the first 43 data points up to $\Psi=34.32°$, from which the data taken at higher tilt angles again deviate systematically. In order to analyze this discrepancy between theory and experiment in more detail, both data sets were divided into subsets, denoted A1 to A5 and B1 to B6, respectively, to each of which the fitting procedure was applied separately. It follows from the results of the partial fits, which are summarized in Table I, that the measurements up to tilt angles of 34° can very well be described by the model defined in Eq. (13). The $(F'_H e^{-W})T_0^{\mathrm{dyn}}$ values derived for the subsets A1 to A3 and B1 agree within their standard deviations and also the

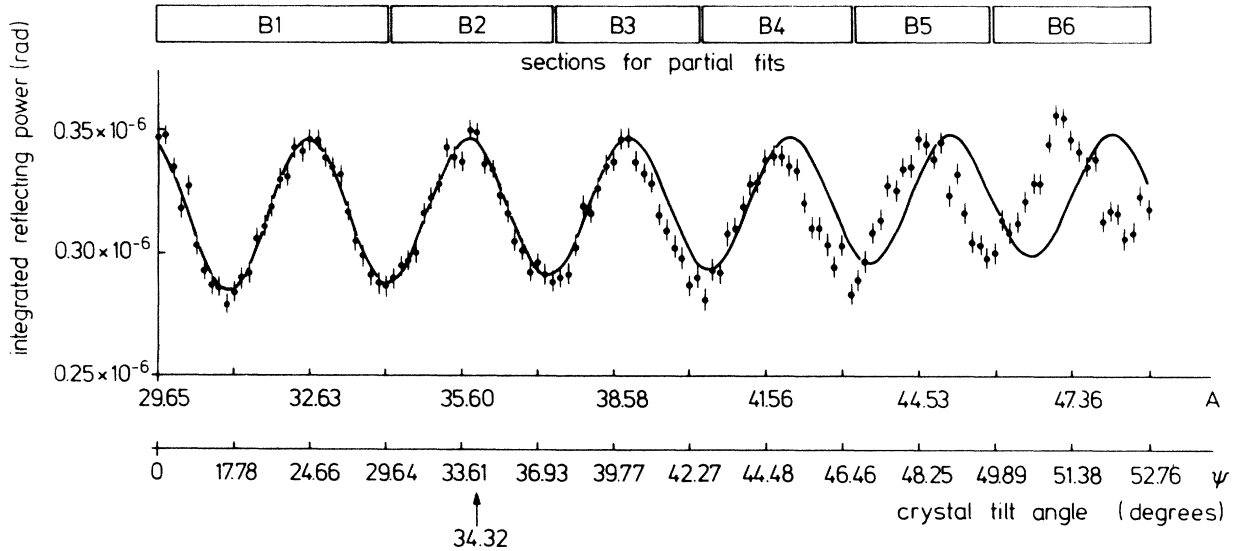

FIG. 7. Integrated reflecting power measured with 0.0265-Å γ radiation at the $(2\bar{2}0)$ reflection of sample I. The solid line represents the final result from the fit of Eq. (13) to 43 data points up to $\Psi=34.32°$ (see caption of Fig. 6).

T_0^{kin} values are in reasonable agreement, bearing in mind that an error of 2% in the scale corresponds to an uncertainty of ± 2.3 and ± 3.3 μm in T_0^{kin} for the long- and the short-wavelength data, respectively, as discussed below. For tilt angles larger than 34° the $(F'_H e^{-W})T_0^{dyn}$ values obtained from the fit increase, which corresponds to a shortening of the Pendellösung period. This is noticeable especially in the small-wavelength data of Fig. 7, where measurements up to high tilt angles were performed in order to obtain an overlap with the A range of the long-wavelength measurement.

In the final fits run to determine structure factors we have therefore used the data of the $(2\bar{2}0)$ reflection up to tilt angles of $\Psi = 34.21°$ and 34.32° for $\lambda = 0.0392$ Å and 0.0265 Å, respectively, which we suppose are not affected significantly by internal strain. The results are listed in Table I together with the results for the partial fits. From the values of the product $(F'_H e^{-W})T_0^{dyn}$ given there, it is straightforward to calculate the (220) structure factor for silicon to

$$F'_{220} = 69.16 \pm 0.03 \quad \text{for } \lambda = 0.0392 \text{ Å},$$

$$F'_{220} = 69.21 \pm 0.06 \quad \text{for } \lambda = 0.0265 \text{ Å}.$$

The $(F'_H e^{-W})T_0^{dyn}$ values have to be divided by T_0^{dyn}, the thickness of the perfect bulk of the crystal, which is obtained by subtracting T_0^{kin} from the measured sample thickness $T_0 = 9.4871(6)$ mm. The Debye-Waller factor e^{-W} was taken from Ref. 6.

The error of 2% in the absolute scale of the experimental data, which leads to an uncertainty of about 9% in μ_0, has been ignored in deriving the standard deviations of the fit parameters quoted in Table I. It is, however, included in the error given for F'_{220}. Calculations with modified data sets reveal that changing the scale factor by $\pm 2\%$ or changing μ_0 by $\pm 9\%$ has a negligible effect on the values of $(F'_H e^{-W})T_0^{dyn}$ and its standard deviation. It is only T_0^{kin} which varies by ± 2.3 and ± 3.3 μm for the longer- and the shorter-wavelength data, respectively. The resulting uncertainty of 40% in T_0^{kin} accounts for about one-half of the error quoted for F'_{220}, the other half being due to the uncertainty in the measurement of the sample thickness T_0 and to the standard deviation of $(F'_H e^{-W})T_0^{dyn}$ derived from the fitting procedure. The calculations also demonstrate that the $(F'_H e^{-W})T_0^{dyn}$ values are not prejudiced by using a fixed value of $F'_H e^{-W}$ in the kinematical scattering term and in the prefactor of the dynamical scattering term, where the structure factor basically acts as a scaling factor. Only T_0^{kin} depends critically on the particular value used for $F'_H e^{-W}$. Since T_0^{kin}, however, constitutes merely a small correction for T_0 and is already subject to an error of 40% in the present measurements, the bias thereby introduced in F'_{220} is not important.

The results obtained from the two different γ lines agree reasonably well, although the shorter-wavelength value is slightly higher. This may be partly due to the limited degree of perfection of the sample. For the comparison of the γ-ray structure factor with the result from x-ray Pendellösung fringe studies of similar accuracy we have chosen the data of Aldred and Hart[6] because the authors also provide experimental values for the Debye-Waller factor which we have used to calculate F'_{220} from $F'_{220}e^{-W}$. In order to simplify this comparison we also used Aldred and Hart's value for the silicon lattice parameter $a_0 = 5.43044$ Å instead of the recently reported more accurate value.[30] The contribution of nuclear Thomson scattering is included in both, x-ray and γ-ray data. The (220) silicon structure factor determined by Aldred and Hart is

$$F'_{220} = 69.21 \pm 0.06 \quad \text{for x rays}$$

and the agreement with the γ-ray values is of the order of $\pm 0.05\%$.

VI. CONCLUDING REMARKS

We have demonstrated that Pendellösung intensity beat measurements on perfect crystals using γ radiation with wavelengths of the order of 0.03 Å allow the determination of structure factors with an accuracy of the order of $\pm 0.05\%$. This result can even be improved, if the transmitted beam is measured with better statistics and if samples of higher perfection can be produced. The agreement with x-ray Pendellösung data is of the same order, which is excellent. One can therefore conclude that Bragg diffraction is very well described by means of the classical Thomson cross section and the form-factor approximation up to photon energies of the order of 450 keV, at least for the low-order reflections in matter not much heavier than silicon. This result may be of more general interest because the γ lines used in the present experiments are at the short-wavelength edge of the spectral distribution of presently available synchrotron radiation.

So far it was well known that γ-ray diffractometry was a powerful tool for studying the degree of perfection of large imperfect crystals by measuring the mosaic distribution function.[18] The present experiments have shown that γ-ray diffraction experiments are also very sensitive to imperfections in almost perfect crystals. To our experience, deviations from conventional dynamical diffraction theory like those found at the (220) reflection, are very common in silicon crystals and it should be emphasized that sample A was the most perfect crystal from a large variety of samples investigated.

ACKNOWLEDGMENTS

The authors thank W.v. Ammon and P. Stallhofer from Wacker-Chemitronic, Burghausen, Federal Republic of Germany (FRG), for providing the silicon samples and for valuable discussions. Thanks are due to N. Mayer and J. Arndt from the Bundesanstalt für Materialprüfung in Berlin for measuring the thickness of the sample and analyzing the quality of its surfaces.

[1]B. W. Batterman and H. Cole, Rev. Mod. Phys. **36**, 681 (1964).
[2]B. K. Tanner, *X-ray Diffraction Topography* (Pergamon, Oxford, 1976).
[3]N. Kato, J. Phys. Soc. Jpn. **18**, 1785 (1963); **19**, 67 (1964); **19**, 971 (1964).
[4]M. Hart, Z. Phys. **189**, 269 (1966).
[5]N. Kato and A. R. Lang, Acta Crystallogr. **12**, 787 (1959).
[6]P. J. E. Aldred and M. Hart, Proc. R. Soc. London, Ser. A **332**, 223 (1973); **332**, 239 (1973).
[7]R. Teworte and U. Bonse, Phys. Rev. B **29**, 2102 (1984).
[8]M. Deutsch and M. Hart, Phys. Rev. B **31**, 3846 (1985).
[9]T. Takama, M. Iwasaki, and S. Sato, Acta Crystallogr. Sect. A **36**, 1025 (1980).
[10]T. Takama and S. Sato, Jpn. J. Appl. Phys. **20**, 1183 (1981).
[11]T. Takama, K. Kobayashi, and S. Sato, Trans. Jpn. Inst. Met. **23**, 153 (1982).
[12]T. Takama and S. Sato, Philos. Mag. B **45**, 615 (1982).
[13]T. Takama, K. Kobayashi, M. Hyugaji, O. Nittono, and S. Sato, Jpn. J. Appl. Phys. **23**, 11 (1984).
[14]T. Takama, N. Noto, K. Kobayashi, and S. Sato, Jpn. J. Appl. Phys. **22**, L304 (1983).
[15]D. Sippel, K. Kleinstück, and G. E. R. Schulze, Phys. Lett. **14**, 174 (1965).
[16]C. G. Shull, Phys. Rev. Lett. **21**, 1585 (1968).
[17]C. G. Shull and J. A. Oberteuffer, Phys. Rev. Lett. **29**, 871 (1972).
[18]J. R. Schneider, in Nuclear Science Applications A, edited by R. Klapisch (Harwood, U.K., 1981), Vol. 2, pp. 227–276.
[19]J. R. Schneider and H. R. Kretschmer, Naturwissenschaften **72**, 191 (1985); **72**, 249 (1985).
[20]J. J. De Marco and R. J. Weiss, Acta Crystallogr. **19**, 68 (1965).
[21]M. Hart and A. R. Lang, Acta Crystallogr. **19**, 73 (1965).
[22]H. Hattori, M. Kuriyama, and N. Kato, J. Phys. Soc. Jpn. **20**, 1047 (1965).
[23]K. Utemisov, V. P. Somenkova, V. A. Somenkov, and S. Sh. Shil'shtein, Kristallografiya **25**, 845 (1980) [Sov. Phys.—Crystallogr. **25(4)**, 484 (1980)].
[24]K. Utemisov, S. Sh. Shil'shtein, and V. A. Somenkov, Kristallografiya **26**, 182 (1981) [Sov. Phys.—Crystallogr. **26(1)**, 101 (1981)].
[25]J. R. Schneider, J. Cryst. Growth **65**, 660 (1983).
[26]J. R. Schneider and H. A. Graf, J. Cryst. Growth **74**, 191 (1986).
[27]J. R. Schneider, H. A. Graf, O. Goncalves, W. von Ammon, P. Stallhofer, and H. Walitzki (unpublished).
[28]Chr. Meixner, Berichte der Kernforschungsanlage Jülich, Report No. 1087-RX (1974) (unpublished).
[29]F. James and M. Roos, Comput. Phys. Commun. **10**, 343 (1975).
[30]P. Becker, P. Seyfried, and H. Siegert, Z. Phys. B **48**, 17 (1982).